

Supporting Information

Highly efficient solar cells based on Cl incorporated tri-cation perovskite materials

*Muhammad Azam^{#,€}, Shizhong Yue^{#,€}, Rui Xu[‡], Kong Liu[€], Kuankuan Ren[€], Yang Sun[€], Jun Liu[€],
Zhijie Wang^{*,€}, Shengchun Qu^{*,€}, Yong lei^{*,‡}, and Zhanguo Wang[€]*

[€]Key Laboratory of Semiconductor Materials Science, Beijing Key Laboratory of Low Dimensional Semiconductor Materials and Devices, Institute of Semiconductors, Chinese Academy of Sciences, Beijing, 100083, People's Republic of China; College of Materials Science and Opto-Electronic Technology, University of Chinese Academy of Sciences, Beijing 100049, China.

E-mail: wangzj@semi.ac.cn, qsc@semi.ac.cn.

[‡]Institut für Physik & IMN MacroNano@ (ZIK), Technische Universität Ilmenau, 98693 Ilmenau, Germany.

E-mail: yong.lei@tu-ilmenau.de.

Section 1 Supporting figures and tables

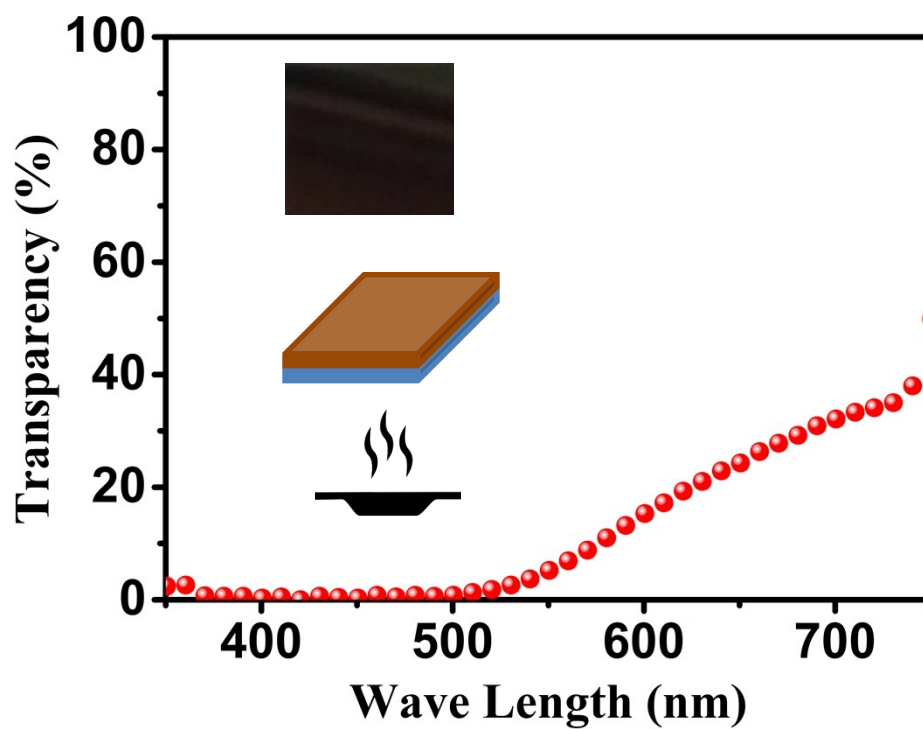


Fig. S1 Transparency of best performing perovskite composition deposited on FTO glass substrate and annealed at 100 °C for 10 min.

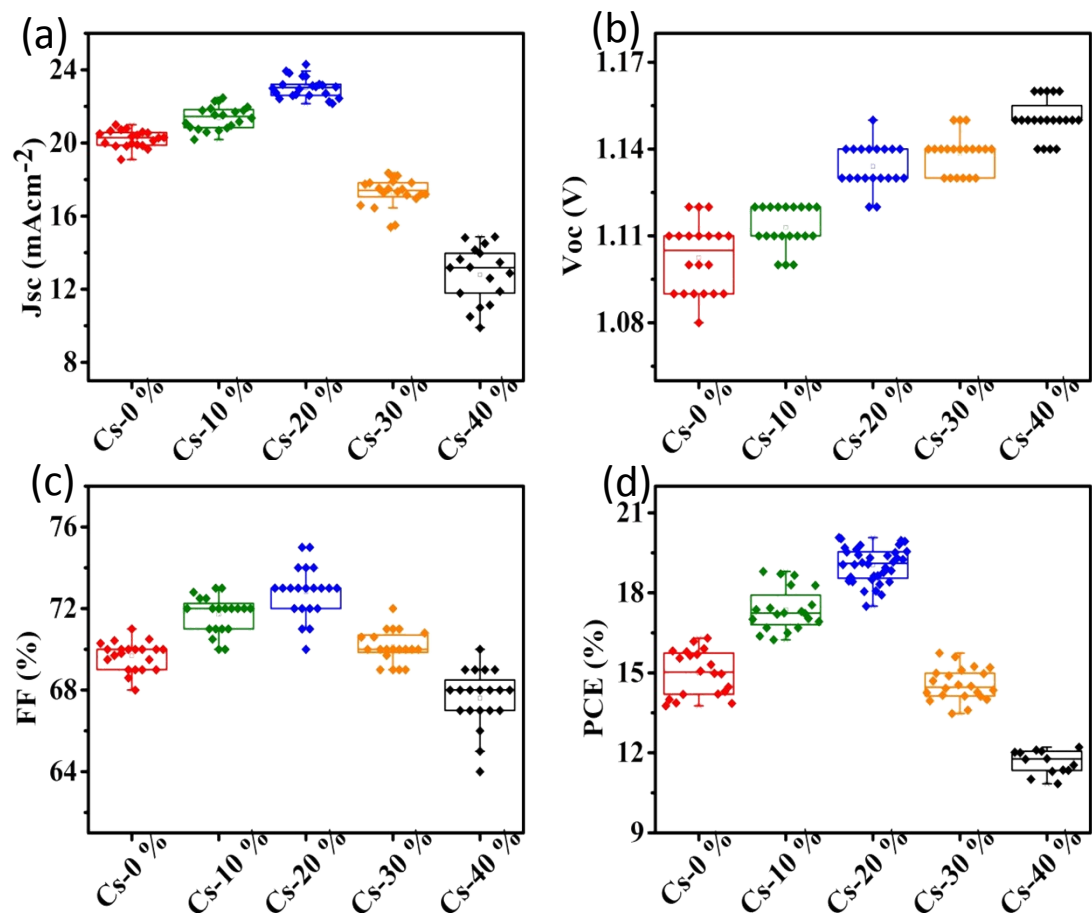


Fig. S2 Statistical analysis of device parameters based on $\text{Cs}_x\text{FA}_{0.2}\text{MA}_{0.8-x}\text{Pb}(\text{I}_{0.9}\text{Cl}_{0.1})_3$ ($x = 0, 0.1, 0.2, 0.3, 0.4$).

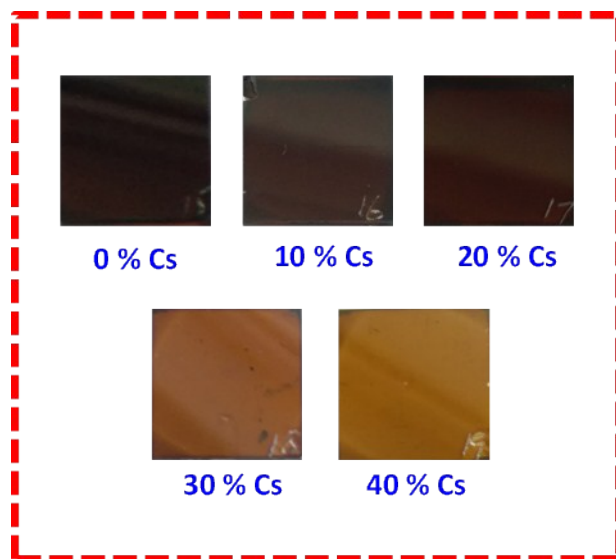


Fig. S3 Colour changes of the perovskite films as the function of Cs ratio in $\text{Cs}_x\text{FA}_{0.4-x}\text{MA}_{0.6}\text{Pb}(\text{I}_{0.9}\text{Cl}_{0.1})_3$ ($x = 0, 0.1, 0.2, 0.3, 0.4$) after annealing at 100 °C for 10 mins.

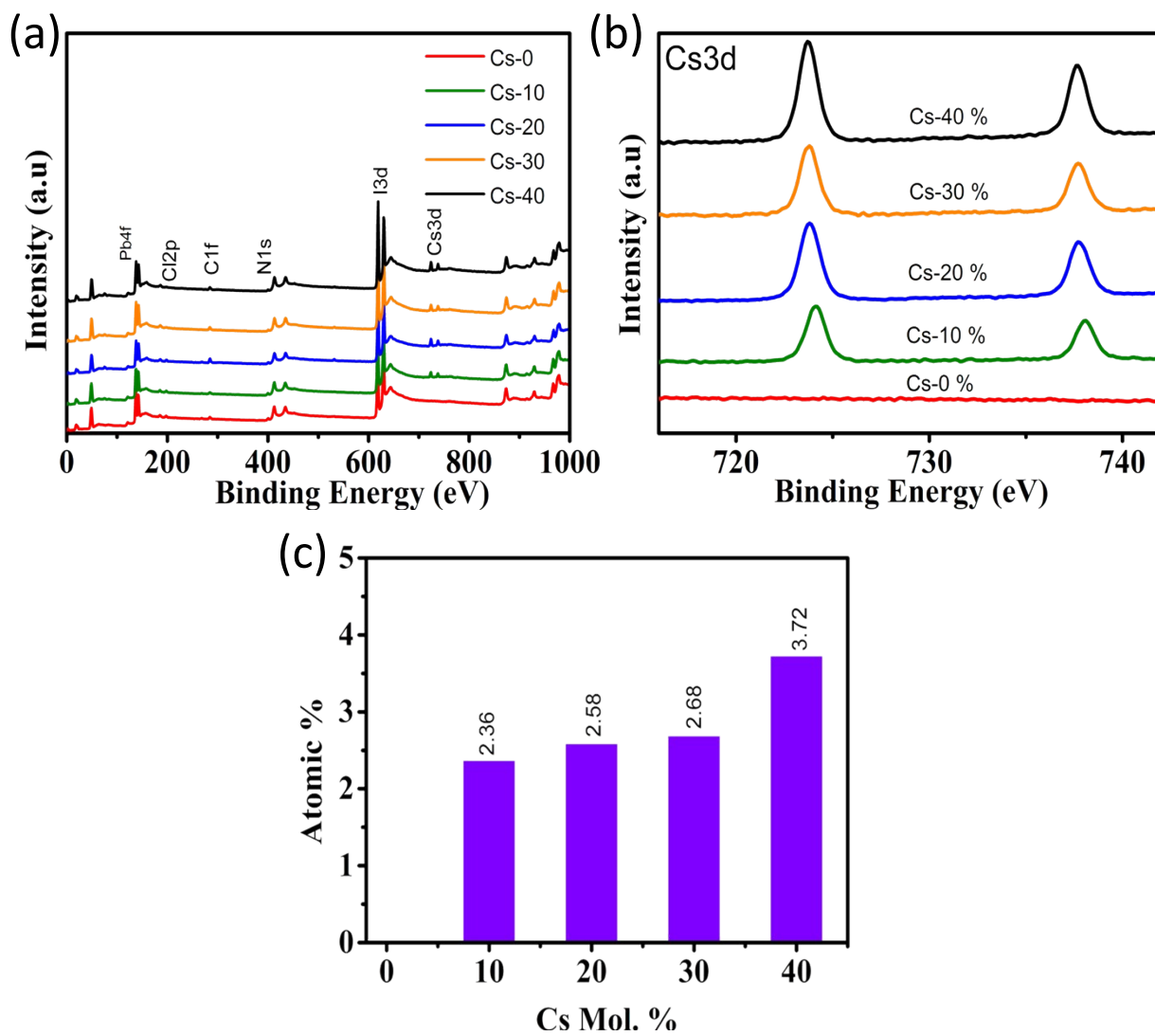


Fig. S4 (a) The X-ray photoelectron spectrum of Cs_xFA_{0.2}MA_{0.8-x}Pb(I_{0.9}Cl_{0.1})₃ (b) XPS spectrum of Cs element. (c) Cs atomic % in respective perovskite films.

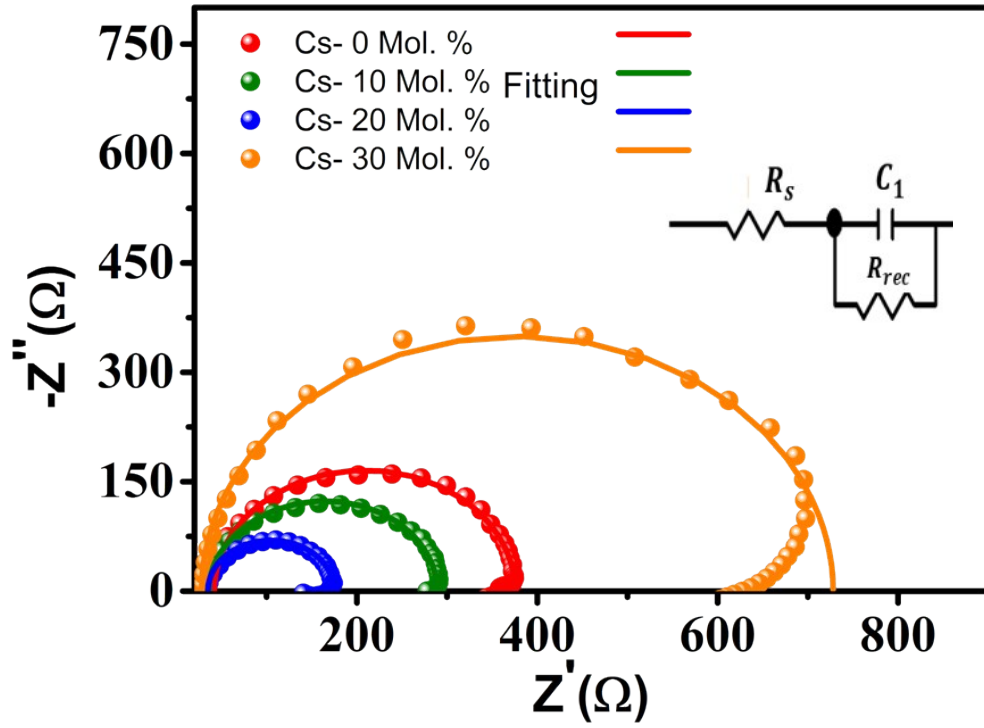


Fig. S5 Nyquist plots of the devices (0-30 Mol.% Cs ratio) measured in dark at $V \approx V_{oc}$, the right inset is the equivalent circuit model.

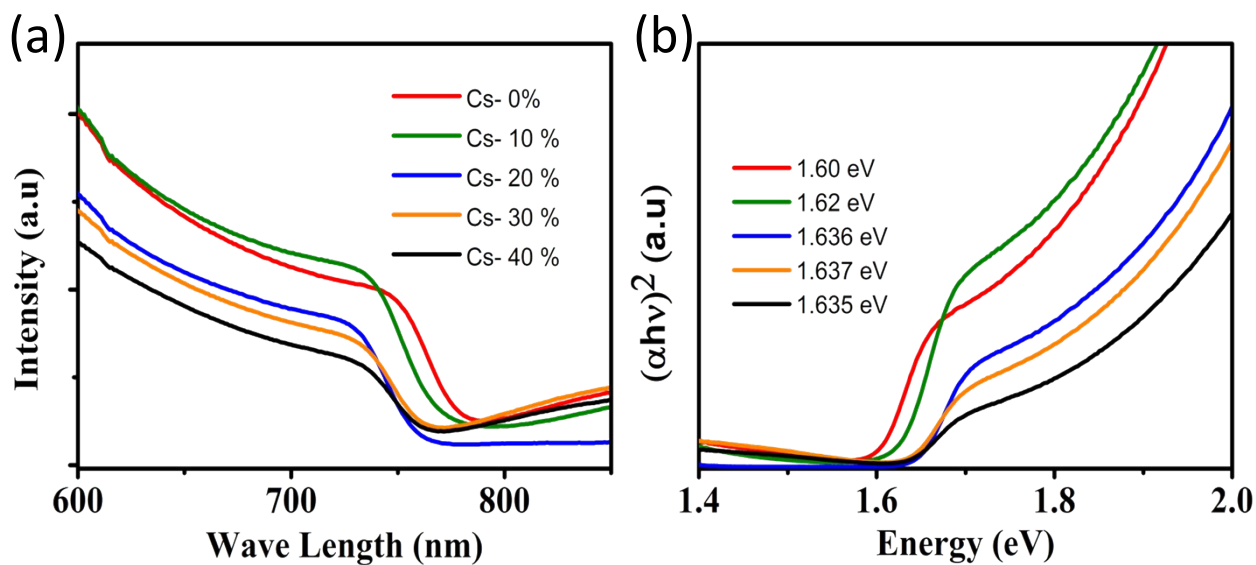


Fig. S6 (a) Absorbance spectra of perovskite films on glass based on perovskite $\text{Cs}_x\text{FA}_{0.2}\text{MA}_{0.8-x}\text{Pb}(\text{I}_{0.9}\text{Cl}_{0.1})_3$ ($x = 0, 0.1, 0.2, 0.3, 0.4$). (b) The corresponding optical band gap energy (E_g).

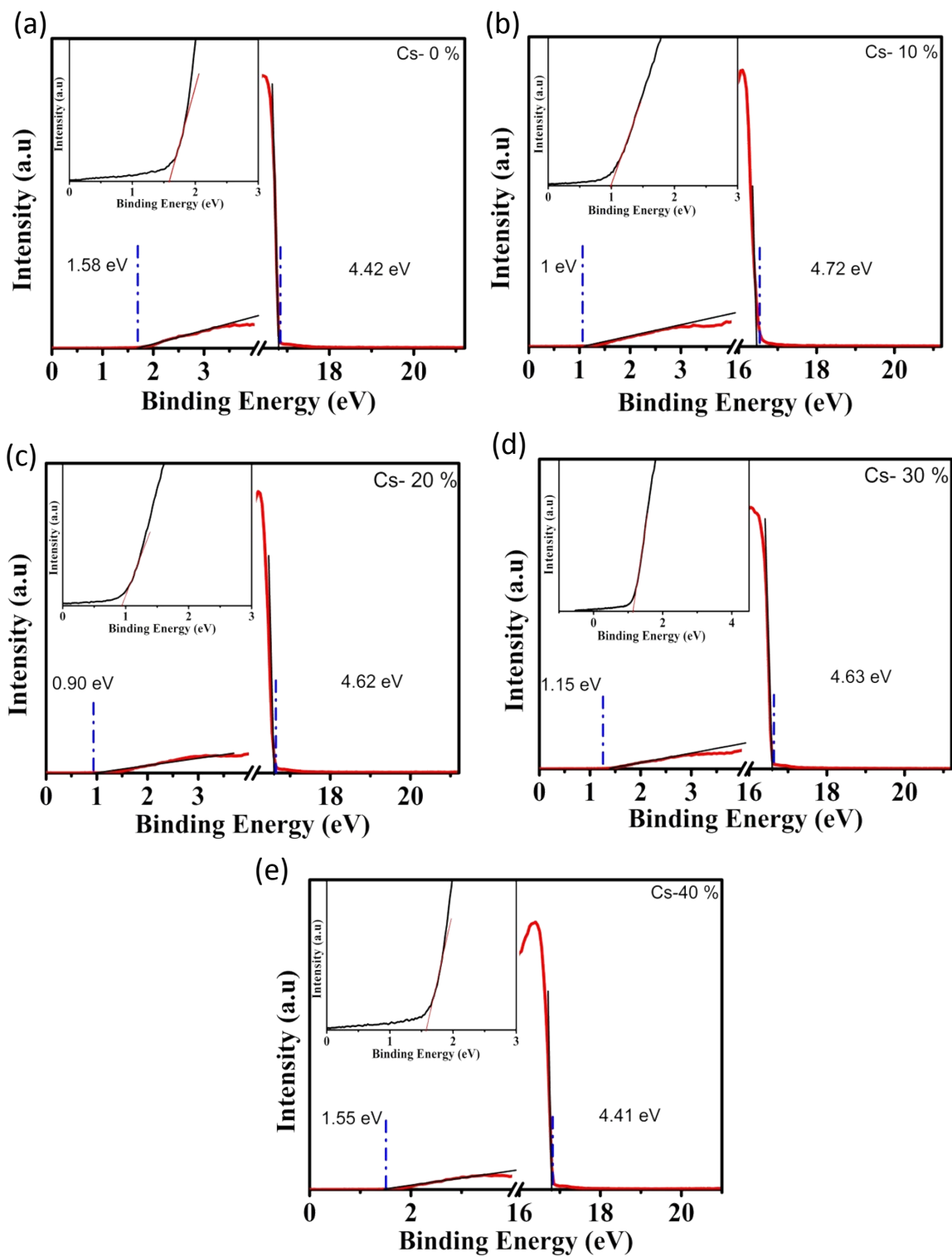


Fig. S7 The ultraviolet photoelectron spectra of series of films, based on $\text{Cs}_x\text{FA}_{0.2}\text{MA}_{0.8-x}\text{Pb}(\text{I}_{0.9}\text{Cl}_{0.1})_3$ the inset zooms in the low binding energy region, (a) $x = 0$ (b) $x = 0.1$ (c) $x = 0.2$ (d) $x = 0.3$ (e) $x = 0.4$

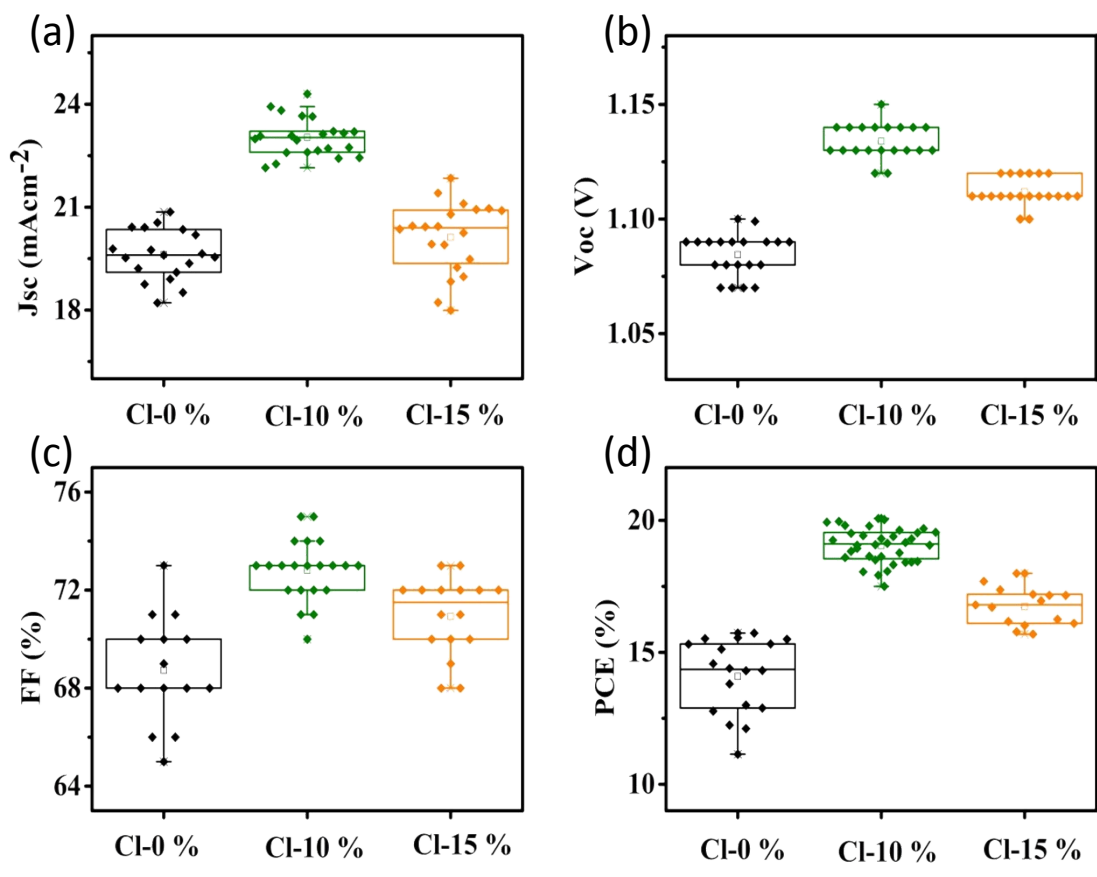


Fig. S8 Statistical analysis of device parameters based on $\text{Cs}_{0.2}\text{FA}_{0.2}\text{MA}_{0.6}\text{Pb}(\text{I}_{1-y}\text{Cl}_y)_3$ ($y = 0, 0.1, 0.15$).

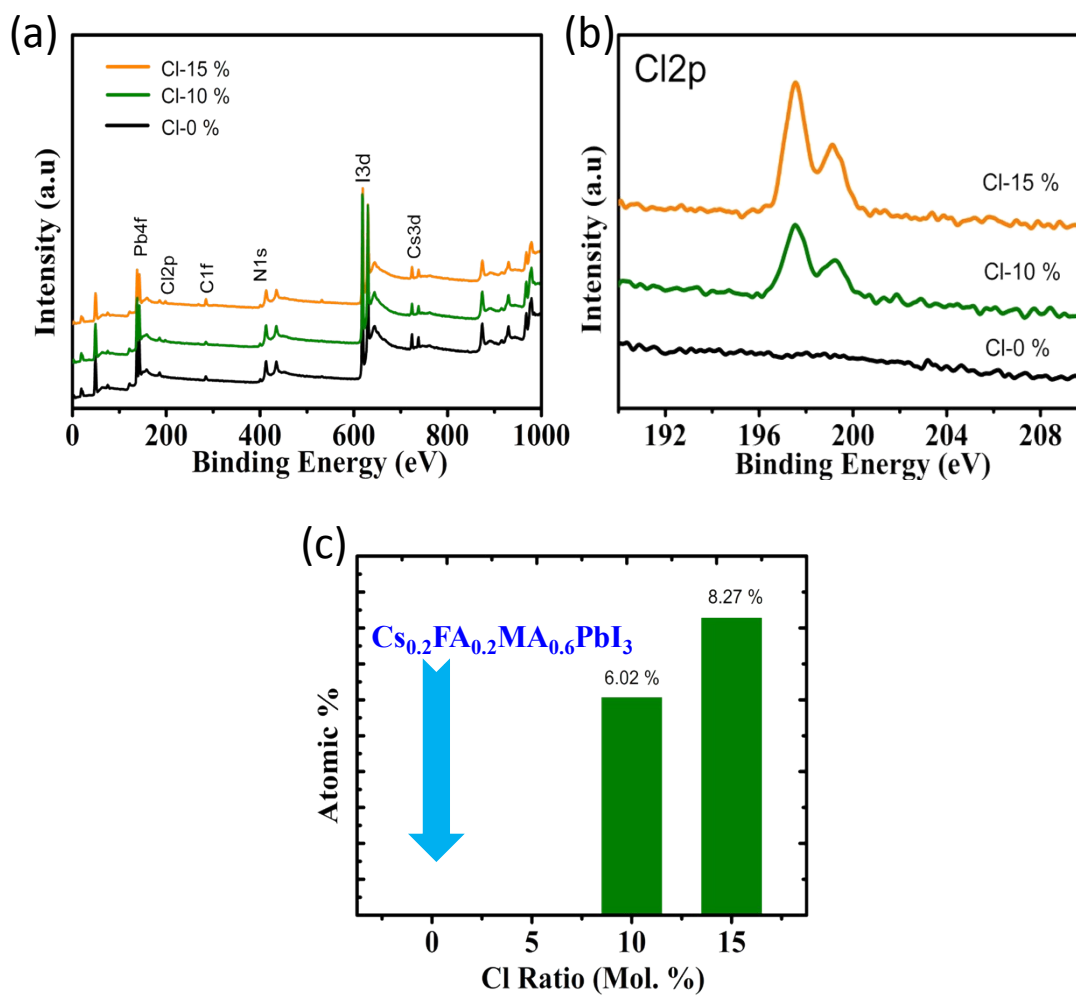


Fig. S9 (a) The X-ray photoelectron spectrum of $\text{Cs}_{0.2}\text{FA}_{0.2}\text{MA}_{0.6}\text{Pb}(\text{I}_{1-y}\text{Cl}_y)_3$ ($y = 0, 0.1, 0.15$) (b) XPS spectrum of Cl element (c) Cl atomic % in respective perovskite films.

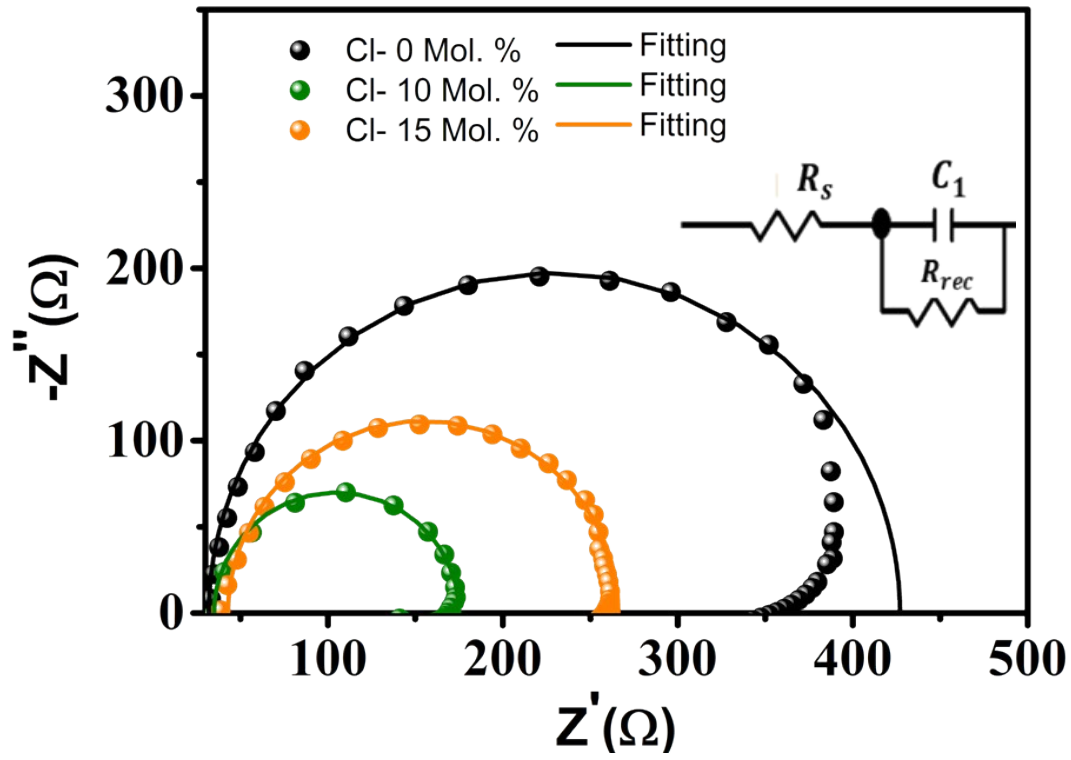


Fig. S10 Nyquist plots of the devices (0-15 Mol.% Cl ratio) measured in dark at $V \approx V_{oc}$, the right inset shows the equivalent circuit.

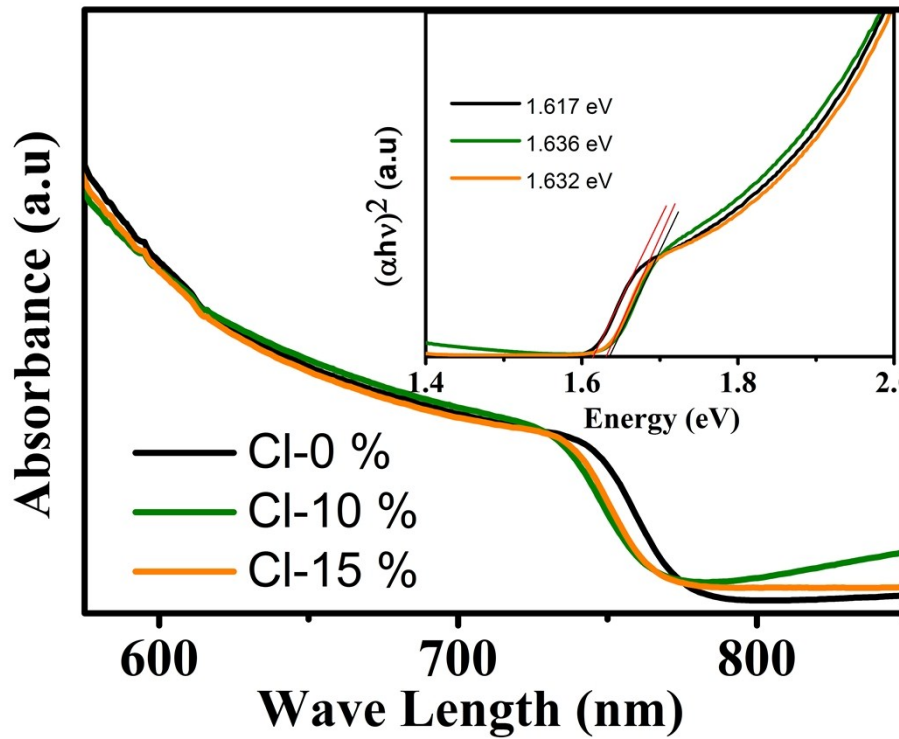


Fig. S11 Absorbance spectra of the perovskite films based on $\text{Cs}_{0.2}\text{FA}_{0.2}\text{MA}_{0.6}\text{Pb}(\text{I}_{1-y}\text{Cl}_y)_3$ ($y = 0, 0.1, 0.15$), the inset shows the Tauc plots to calculate the band gap energy of corresponding films.

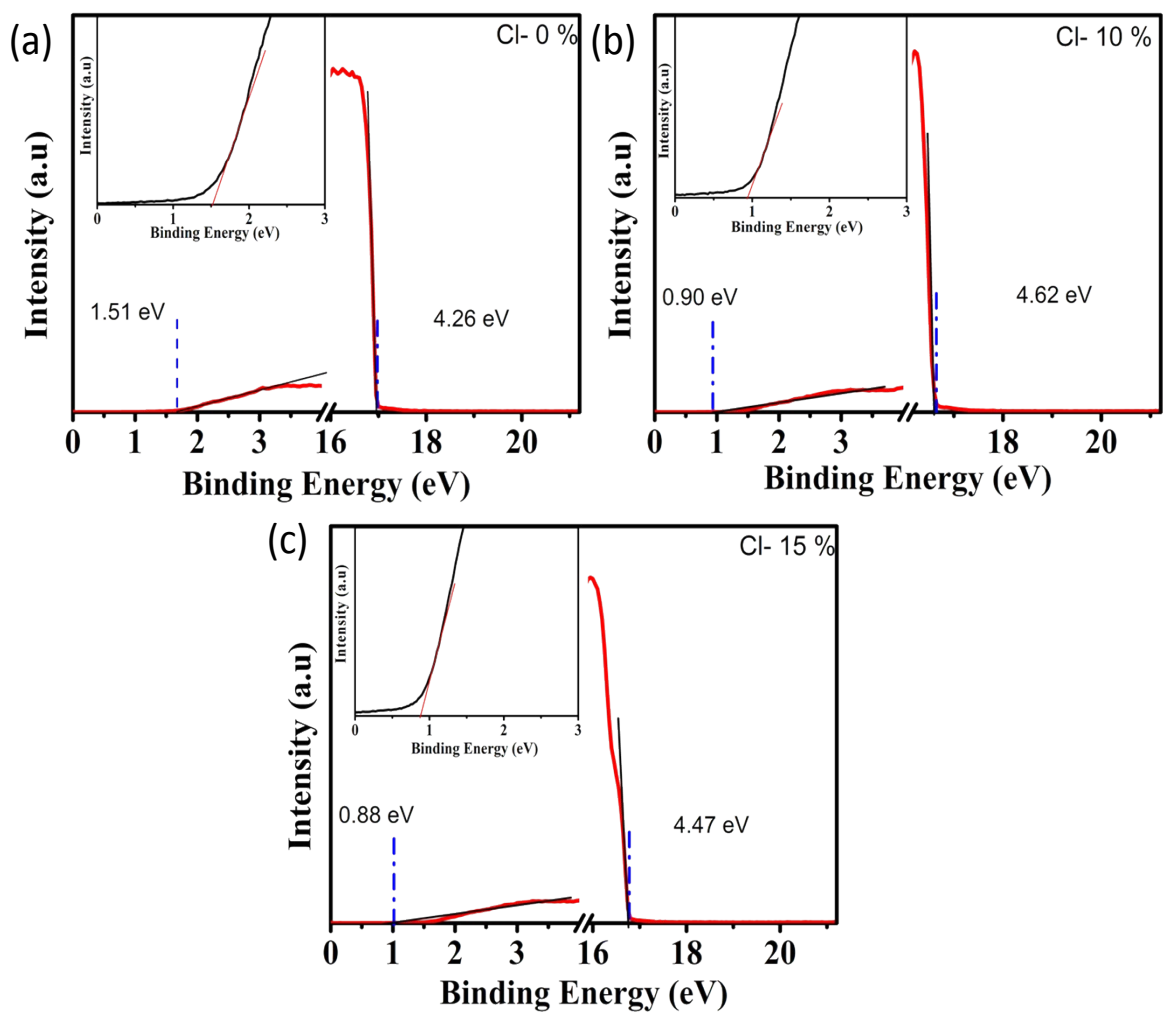


Fig. S12 The ultraviolet photoelectron spectra of series of films, based on $\text{Cs}_{0.2}\text{FA}_{0.2}\text{MA}_{0.6}\text{Pb}(\text{I}_{1-y}\text{Cl}_y)_3$, the inset zooms in the low binding energy region, (a) $y = 0$ (b) $y = 0.1$ (c) $y = 0.15$

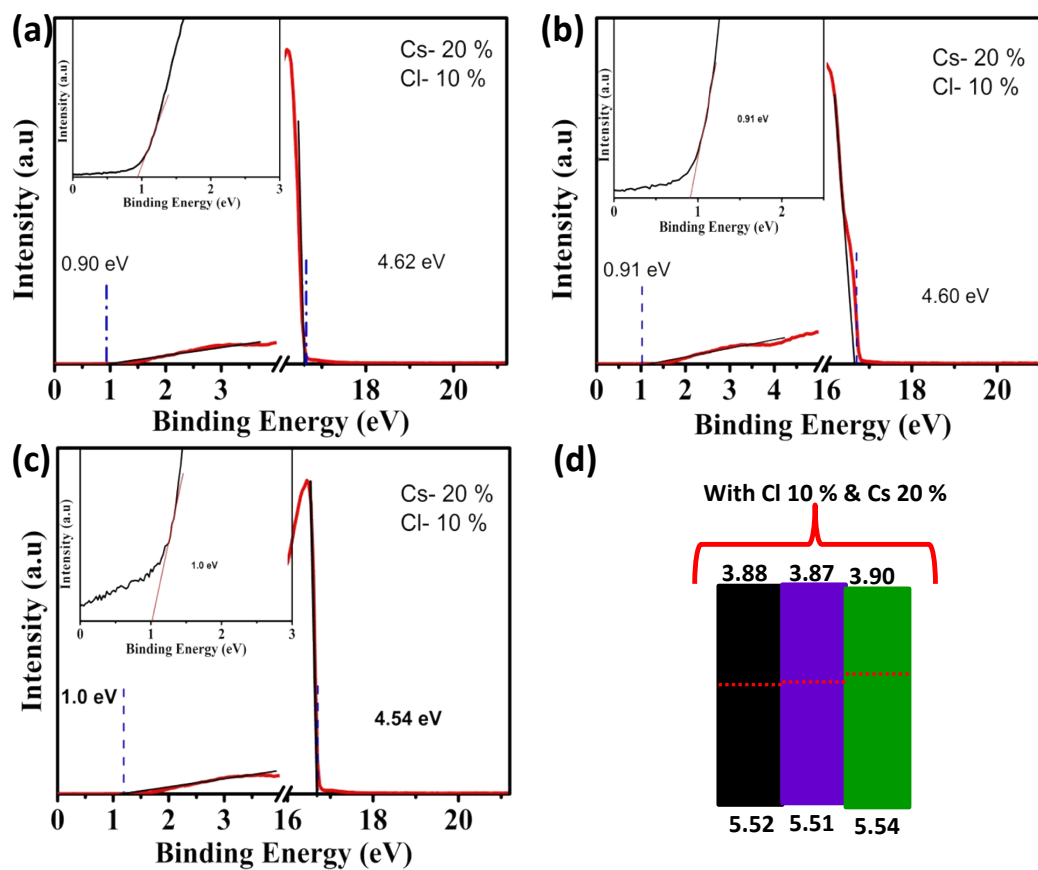


Fig. S13 UPS spectra of the $\text{Cs}_x\text{FA}_{0.2}\text{MA}_{0.8-x}\text{Pb}(\text{I}_{1-y}\text{Cl}_y)_3$ film with 20% Cs and 10% Cl incorporation (a-c). (d) Energy level diagram for all three perovskite (10% Cl, 20% Cs) films.

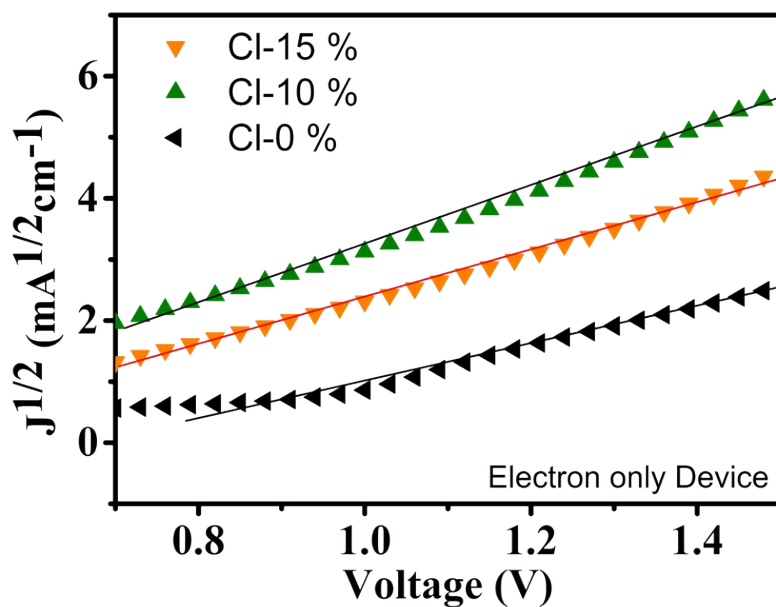


Fig. S14 $J^{1/2}$ - V curves of the electron-only devices with the structure of ITO/Al/ $\text{Cs}_{0.2}\text{FA}_{0.2}\text{MA}_{0.6}\text{Pb}(\text{I}_{1-y}\text{Cl}_y)_3$ ($y = 0, 0.1, 0.15$)/ PC_{61}BM /Al.

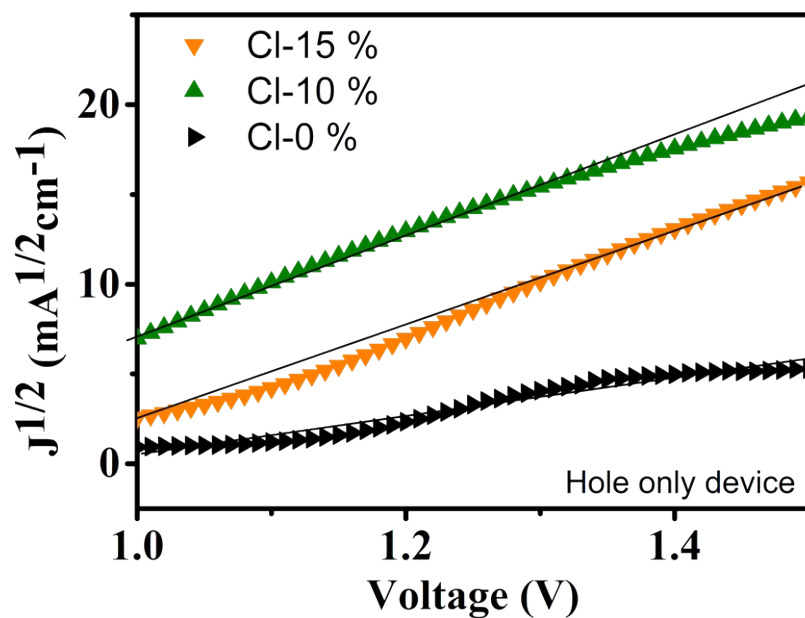


Fig. S15 $J^{1/2}$ - V curves of the Hole-only devices with the structure of ITO/ $\text{NiO}_x+5\%\text{Cu}$ / $\text{Cs}_{0.2}\text{FA}_{0.2}\text{MA}_{0.6}\text{Pb}(\text{I}_{1-y}\text{Cl}_y)_3$ ($y = 0, 0.1, 0.15$)/Au.

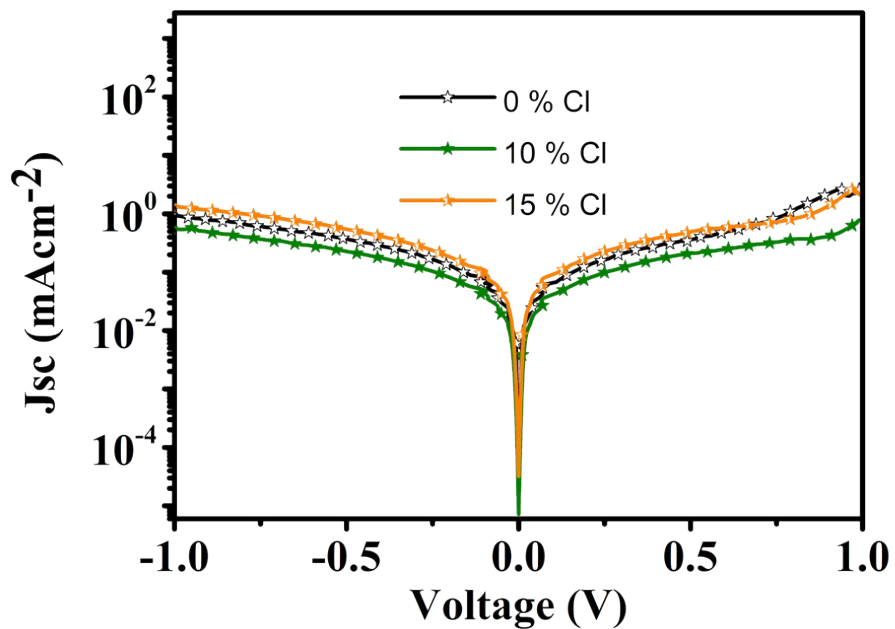


Fig. S16 J–V curves of the devices measured under dark conditions based on $\text{Cs}_{0.2}\text{FA}_{0.2}\text{MA}_{0.6}\text{Pb}(\text{I}_{1-y}\text{Cl}_y)_3$ ($y = 0, 0.1, 0.15$) perovskite material.

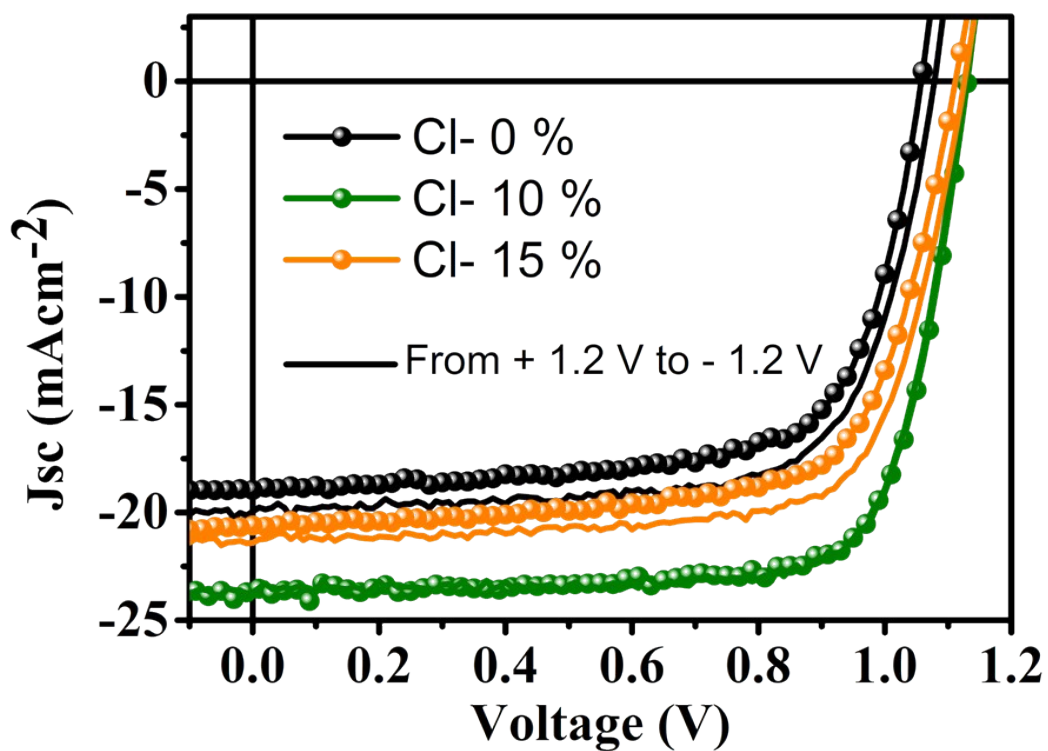


Fig. S17 J-V characteristics of the devices fabricated by perovskite Films $\text{Cs}_{0.2}\text{FA}_{0.2}\text{MA}_{0.6}\text{Pb}(\text{I}_{1-y}\text{Cl}_y)_3$ ($y = 0, 0.1, 0.15$) measured in forward and reverse scan direction.

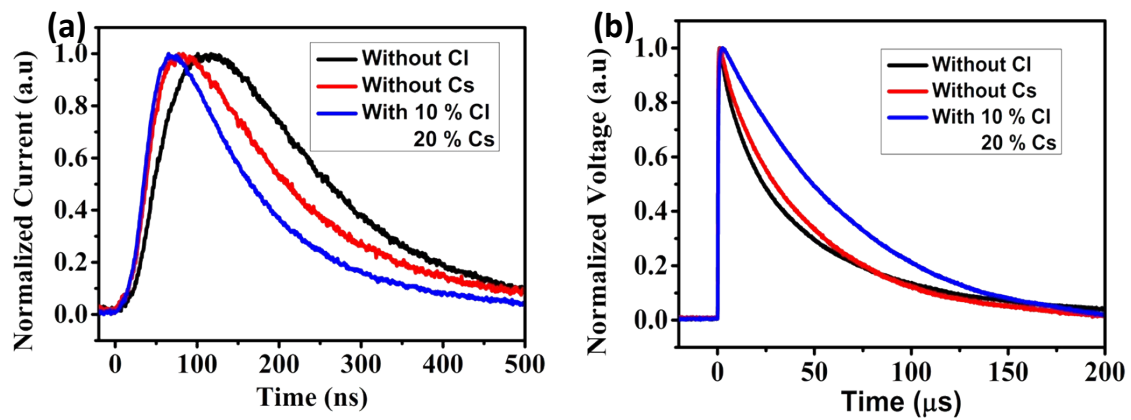


Fig. S18 (a) Transient photocurrent decay curves with and without Cs, Cl incorporation. (b) Transient photo voltage decay curves of corresponding devices.

Table S1 The fitting result of impedance spectra for the devices based on $\text{Cs}_x\text{FA}_{0.2}\text{MA}_{0.8-x}\text{Pb}(\text{I}_{0.9}\text{Cl}_{0.1})_3$ ($x = 0, 0.1, 0.2, 0.3$) films.

Cs [Mol. %]	Rs [Ω]	R1 [Ω]	R2 [Ω]
0	42	292	41.5
10	37	217	33
20	35	120	20
30	28	600	100

Table S2 The fitting result of impedance spectra for the devices based on $\text{Cs}_{0.2}\text{FA}_{0.2}\text{MA}_{0.6}\text{Pb}(\text{I}_{1-y}\text{Cl}_y)_3$ ($y = 0, 0.1, 0.15$) films.

Cl Mol. %	Rs [Ω]	R1 [Ω]	R2 [Ω]
0	35	325	70
10	35	120	20
15	43	188	35

Table S3 The V_{TFL} and electron trap-states of the corresponding electron-only devices.

Electron only device	CI-0 [M%]	CI-10 [M%]	CI-15 [M%]
V_{TFL} [V]	0.92	0.43	0.5
n_t [$10^{16}cm^{-3}$]	2.17	1.01	1.18

Table S4 The V_{TFL} and hole trap-states of the corresponding hole-only devices.

Hole only device	CI-0	CI-10	CI-15
V_{TFL} [V]	1.04	0.66	0.83
n_t [$10^{16}cm^{-3}$]	2.45	1.55	1.95

Table S5 The electron mobility of the corresponding electron-only devices.

Electron Mobility	CI-0	CI-10	CI-15
$10^{-4}cm^2V^{-1}s^{-1}$	0.66	1.68	1.04

Table S6 The hole mobility of the corresponding hole-only devices.

Hole Mobility	CI-0	CI-10	CI-15
$10^{-3}cm^2V^{-1}s^{-1}$	1.22	5.90	4.09

Table S7 Corresponding device parameters measured under reverse and forward scan directions.

Cl Ratio	Scan	J_{sc}	V_{oc}	FF	PCE
[Mol. %]		[mAcm⁻²]	[V]	[%]	[%]
0	Forward	19.95	1.079	70	15.15
	Reverse	18.96	1.059	69	14.03
10	Reverse	23.67	1.13	75	20.24
	Forward	23.72	1.13	75	20.30
15	Forward	21.41	1.12	71	17.38
	Reverse	20.60	1.11	70	16.11

Section 2

Discussion on derivation of the integrated J_{sc} from IPCE spectra with J_{sc} from J-V curve

The integrated J_{sc} from IPCE is acceptably lower than the J_{sc} from J-V curve, due to the following reasons:

(1) For the standard measurement of J-V curves, the light intensity is 100 mW/cm^2 . In the IPCE measurement, the light from the monochromator is usually weaker than from the AM1.5 light source (100 mW/cm^2). The relevant calculated current is obtained from integrated IPCE spectra and the consideration of light from the AM1.5 light source. Due to the fact that relationship of photocurrents and light intensities is not strictly linear, such variation is normal.

(2) The J-V curves are measured in glove box protected by N_2 , while the IPCE spectra are measured in air. Though the stabilities of our devices are improved particularly in N_2 , the sensitivity of the device to H_2O is not completely eliminated. The water molecule in air causes the slight decay of the photovoltaic performance.